J|A|C|S
ARTICLES
Published on Web 03/04/2004

Probing the Transition States of Four Glucoside Hydrolyses with ^{13}C Kinetic Isotope Effects Measured at Natural Abundance by NMR Spectroscopy

Jason K. Lee,[†] Alex D. Bain,[†] and Paul J. Berti*[,†,‡,§]

Contribution from the Department of Chemistry, Department of Biochemistry, and the Antimicrobial Research Centre, McMaster University, 1280 Main Street West, Hamilton, Ontario, L8S 4M1, Canada

Received November 3, 2003; E-mail: berti@mcmaster.ca

Abstract: Kinetic isotope effects (KIEs) were measured for methyl glucoside (**4**) hydrolysis on unlabeled material by NMR. Twenty-eight ^{13}C KIEs were measured on the acid-catalyzed hydrolysis of **α-4** and ***β*-4**, as well as enzymatic hydrolyses with yeast α-glucosidase and almond β-glucosidase. The 1-^{13}C KIEs on the acid-catalyzed reactions of **α-4** and ***β*-4**, 1.007(2) and 1.010(6), respectively, were in excellent agreement with the previously reported values (1.007(1), 1.011(2): Bennet and Sinnott, *J. Am. Chem. Soc.* **1986**, *108*, 7287). Transition state analysis of the acid-catalyzed reactions using the ^{13}C KIEs, along with the previously reported ^{2}H KIEs, confirmed that both reactions proceed with a stepwise $D_N{}^*A_N$ mechanism and showed that the glucosyl oxocarbenium ion intermediate exists in an E_3 sofa or $^4H_3$ half-chair conformation. ^{13}C KIEs showed that the α-glucosidase reaction also proceeded through a $D_N{}^*A_N$ mechanism, with a 1-^{13}C KIE of 1.010(4). The secondary ^{13}C KIEs showed evidence of distortions in the glucosyl ring at the transition state. For the β-glucosidase-catalyzed reaction, the 1-^{13}C KIE of 1.032(1) demonstrated a concerted A_ND_N mechanism. The pattern of secondary ^{13}C KIEs was similar to the acid-catalyzed reaction, showing no signs of distortion. KIE measurement at natural abundance makes it possible to determine KIEs much more quickly than previously, both by increasing the speed of KIE measurement and by obviating the need for synthesis of isotopically labeled compounds.

The outlines of glycoside hydrolysis have been clear for some time.[1−5] The details remain the subject of intense interest, particularly with regard to how enzymes manipulate conformation, structure, and reactivity to achieve catalysis. Determining the transition states (TSs)[6] of these reactions is important for understanding catalysis in atomic detail, and for designing TS mimics as inhibitors, potentially with pharmaceutical applications.

Kinetic isotope effects (KIEs) are a uniquely powerful means of probing TSs.[5,7−9] Multiple (or families of) KIEs define TS structures. In the best cases, it has been possible to determine the structures of TSs with accuracy that rivals that of X-ray crystallography of stable molecules.[10] KIEs reflect changes in atoms' vibrational environments between the reactant and the TS. A less restrained environment resulting from decreased bond strengths or changes in bond angles gives normal KIEs (i.e., the light atom reacts more quickly than the heavy atom, $^{light}k/^{heavy}k > 1$). A more constrained environment gives inverse KIEs, $^{light}k/^{heavy}k < 1$. KIEs measured at many locations in the reactant provide sufficient information to make specific, quantitative statements about TS structures.

The practical challenges in determining KIEs are significant in terms of both synthesizing isotopically labeled molecules and the KIE measurement itself. Both challenges were addressed in 1995 when Singleton and co-workers[11] showed that it was possible to measure multiple, high precision ^{2}H and ^{13}C KIEs by NMR on a Diels−Alder reaction (Scheme 1) with natural abundance (unlabeled) reactants. When reactions are taken almost to completion, the residual reactant becomes highly enriched in the slower reacting isotopomers.[12] It is this enrichment that is detected by NMR. ^{2}H, ^{13}C, and ^{17}O KIEs have been measured on a variety of reactions, and several groups have adopted the method,[13−23] but it had not been applied to enzymatic reactions until now.

[†] Department of Chemistry.
[‡] Department of Biochemistry.
[§] Antimicrobial Research Centre.

(1) Capon, B. *Chem. Rev.* **1969**, *69*, 407.
(2) Jencks, W. P. *Acc. Chem. Res.* **1980**, *13*, 161.
(3) Sinnott, M. L. *Chem. Rev.* **1990**, *90*, 1171.
(4) Zechel, D. L.; Withers, S. G. *Acc. Chem. Res.* **2000**, *33*, 11.
(5) Berti, P. J.; Tanaka, K. S. E. *Adv. Phys. Org. Chem.* **2002**, *37*, 239.
(6) Abbreviations: DFT, density functional theory; EIE, equilibrium isotope effect; FID, free induction decay; KIE, kinetic isotope effect; TS, transition state.
(7) Schramm, V. L. *Acc. Chem. Res.* **2003**, *36*, 588.
(8) Schramm, V. L. *Curr. Opin. Chem. Biol.* **2001**, *5*, 556.
(9) Schramm, V. L. *Annu. Rev. Biochem.* **1998**, *67*, 693.
(10) Scheuring, J.; Berti, P. J.; Schramm, V. L. *Biochemistry* **1998**, *37*, 2748.
(11) Singleton, D. A.; Thomas, A. A. *J. Am. Chem. Soc.* **1995**, *117*, 9357.
(12) **4** and [1-^{13}C]**4** are isotopologues of each other; [1-^{13}C]**4** and [2-^{13}C]**4** are isotopomers.
(13) Singleton, D. A.; Merrigan, S. R.; Liu, J.; Houk, K. N. *J. Am. Chem. Soc.* **1997**, *119*, 3385.
(14) Singleton, D. A.; Hang, C.; Szymanski, M. J.; Meyer, M. P.; Leach, A. G.; Kuwata, K. T.; Chen, J. S.; Greer, A.; Foote, C. S.; Houk, K. N. *J. Am. Chem. Soc.* **2003**, *125*, 1319.
(15) Singleton, D. A.; Nowlan, D. T., III; Jahed, N.; Matyjaszewski, K. *Macromolecules* **2003**, *36*, 8609.

Scheme 1

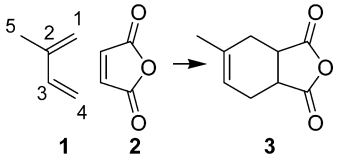

1 **2** **3**

In this study, we measured ^{13}C KIEs on acid- and enzyme-catalyzed hydrolyses of α- and *β*-methyl glucopyranosides (**α-4** and ***β*-4**). The enzymatic hydrolyses studied here employed yeast α-glucosidase[24,25] and almond *β*-glucosidase.[26−29] Both are retaining glycosidases that operate through a double-displacement mechanism with a covalent acylal intermediate. The product glucose (**5**) has the same anomeric configuration as the reactant (Figure 1).[3,4]

Glycoside hydrolysis mechanisms tread the borderline between highly dissociative A_ND_N[30] (S_N2) and true stepwise $D_N{*}A_N$ or $D_N + A_N$ (S_N1) mechanisms.[1−5] In all cases, the TSs have significant oxocarbenium ion character. In A_ND_N mechanisms, the TS is oxocarbenium ion-like (**6**), while a discrete oxocarbenium ion intermediate is formed in a $D_N{*}A_N$ mechanism (**7**). Primary ^{13}C KIEs can be used to distinguish between these mechanisms, being larger for an A_ND_N mechanism, 1.02−1.06, than for a stepwise mechanism, ≤1.01.[5,9,31]

Bennet and Sinnott measured ^2H, ^{13}C, and ^{18}O KIEs for acid-catalyzed **α-4** and ***β*-4** hydrolyses.[32] The 1-^{13}C KIEs indicated stepwise mechanisms. They concluded that the **α-4** TS had a flattened $^1S_3$ ring conformation while ***β*-4** was a $^4C_1$ chair flattened toward a $^4H_3$ half-chair.

Materials and Methods

α− and *β*-methyl glucoside (**α-4** and ***β*-4**) were from Sigma. Perchloric acid (trace metal grade, 67−71% assay), pyridine (anhydrous, 99.8%), and acetic anhydride (99+%) were from Aldrich. d_6-Acetone (99.9%) and D_2O (99%) were from Cambridge Isotope Laboratories. All other reagents were analytical or biotech grade from Aldrich, Sigma, or Bioshop (Burlington, ON). Thin-walled 5 mm NMR tubes (Wilmad 507 PP) were used. Sealed NMR tubes were made by adding an 8 cm extension of 6 mm o.d. glass tubing to a regular NMR tube.

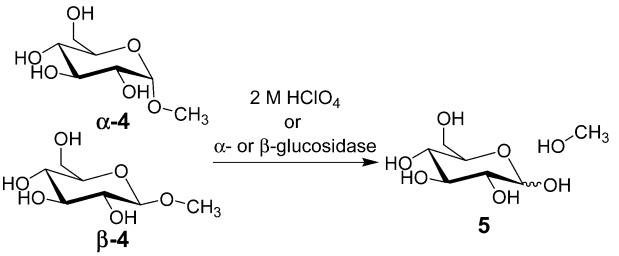

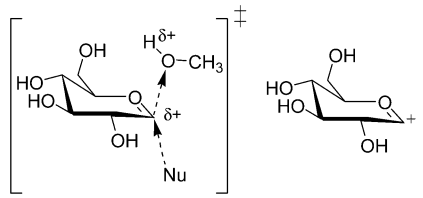

6 **7**

The following enzymes were from Sigma: glucose oxidase (Type X-S from *Aspergillus niger*), bovine liver catalase, baker's yeast α-glucosidase (EC 3.2.1.20), recombinant *Saccharomyces cerevisiae* α-glucosidase (EC 3.2.1.20), and almond *β*-glucosidase (EC 3.2.1.21). Baker's yeast α-glucosidase was described as partially purified. The protein purity, estimated by SDS/10% PAGE, was ∼20% (data not shown). The fact that many glucosidases do not act on **4** (refs 33,34 and unpublished data), coupled with the fact that KIEs with recombinant and partially pure enzymes were indistinguishable (see Supporting Information), argues that α-glucosidase was responsible for all of the observed hydrolysis of **α-4**. Almond *β*-glucosidase is also described as partially purified, but was >90% pure on SDS/10% PAGE (data not shown) with a molecular weight of ∼90 kDa. Thus, it appeared to be essentially pure isozyme B, as was previously observed for this source.[27−29]

Reducing Sugar Assay. The reducing sugar assay,[35] which detects glucose, was used for routine kinetics measurements and for determining the approximate extents of reaction for KIE reactions while they were in progress.

Enzyme Kinetics. Steady-state kinetic parameters were determined at 25 °C for **α-** and ***β*-4** with recombinant α-glucosidase or almond *β*-glucosidase in 50 mM potassium phosphate buffer, pH 6.8, 1 mM EDTA, 1 mg/mL bovine serum albumin, in 1 mL. Reactions were performed with [**α-4**] = 5−500 mM with 0.1 mg/mL (2.8 U/mL) α-glucosidase or [***β*-4**] = 20−500 mM with 0.125 mg/mL (1.55 U/mL) *β*-glucosidase.

Reactions for KIE Measurement. Acid-Catalyzed Hydrolyses. Acid-catalyzed **4** hydrolyses were performed essentially as described previously,[32] but on a 1000 mL scale. A 200 mL solution of 190 mM **4** and 25 mM sodium succinate (internal standard for determining extent of reaction) in 2 M $HClO_4$ was prepared; 5 mL was removed to measure the extent of reaction at $t = 0$, and the rest was added to 800 mL of 2 M $HClO_4$ preheated to 80 °C. Reactions were run ca. 8.5 h (**α-4**) or ca. 4 h (***β*-4**). Reactions were followed with the reducing sugar assay and stopped at ∼90% completion by cooling on ice and neutralizing with 2 M KOH, with continued cooling on ice. Precipitated $KClO_4$ was removed by filtration, and the filtrate was divided between two 1 L Erlenmeyer flasks and diluted to a final volume of 600 mL each.

Enzymatic Hydrolyses. Enzymatic reactions (300 mL) contained 100 mM **4**, 50 mM potassium phosphate, pH 6.8, 1 mM EDTA, 1 mg/mL bovine serum albumin, 30 *μ*g/mL kanamycin, 50 *μ*g/mL

(16) Singleton, D. A.; Hang, C.; Szymanski, M. J.; Greenwald, E. E. *J. Am. Chem. Soc.* **2003**, *125*, 1176.
(17) Saettel, N. J.; Wiest, O.; Singleton, D. A.; Meyer, M. P. *J. Am. Chem. Soc.* **2002**, *124*, 11552.
(18) Singleton, D. A.; Merrigan, S. R.; Kim, B. J.; Beak, P.; Phillips, L. M.; Lee, J. K. *J. Am. Chem. Soc.* **2000**, *122*, 3296.
(19) Singleton, D. A.; Merrigan, S. R. *J. Am. Chem. Soc.* **2000**, *122*, 11035.
(20) Frantz, D. E.; Singleton, D. A. *J. Am. Chem. Soc.* **2000**, *122*, 3288.
(21) Yi, C. S.; Yun, S. Y.; He, Z. J. *Organometallics* **2003**, *22*, 3031.
(22) Griesbeck, A. G.; Bondock, S.; Cygon, P. *J. Am. Chem. Soc.* **2003**, *125*, 9016.
(23) Corey, E. J.; Noe, M. C.; Grogan, M. J. *Tetrahedron Lett.* **1996**, *37*, 4899.
(24) Hong, S. H.; Marmur, J. *Gene* **1986**, *41*, 75.
(25) McCarter, J. D.; Withers, S. G. *J. Biol. Chem.* **1996**, *271*, 6889.
(26) He, S.; Withers, S. G. *J. Biol. Chem.* **1997**, *272*, 24864.
(27) Dale, M. P.; Kopfler, W. P.; Chait, I.; Byers, L. D. *Biochemistry* **1986**, *25*, 2522.
(28) Legler, G.; Hasnain, S. N. *Hoppe-Seyler's Z. Physiol. Chem.* **1970**, *351*, 25.
(29) Helferich, B.; Kleinschmidt, T. *Hoppe-Seyler's Z. Physiol. Chem.* **1968**, *349*, 25.
(30) According to IUPAC nomenclature, a reaction mechanism is divided into elementary steps, with A_N representing nucleophilic addition and D_N representing nucleophilic dissociation. A bimolecular (S_N2) reaction is represented as A_ND_N. $D_N{*}A_N$ and $D_N{+}A_N$ mechanisms are stepwise (S_N1), with a discrete intermediate formed between leaving group departure and nucleophile approach. The signs "*" or "+" denote, respectively, an intermediate too short-lived for the leaving group to diffuse into solution or one that is long-lived enough to diffusionally equilibrate with solvent. (Guthrie, R. D.; Jencks, W. P. *Acc. Chem. Res.* **1989**, *22*, 343.).
(31) Chen, X.-Y.; Berti, P. J.; Schramm, V. L. *J. Am. Chem. Soc.* **2000**, *122*, 6527.
(32) Bennet, A. J.; Sinnott, M. L. *J. Am. Chem. Soc.* **1986**, *108*, 7287.
(33) Matsusaka, K.; Chiba, S.; Shimomura, T. *Agric. Biol. Chem.* **1977**, *41*, 1917.
(34) Khan, N. A.; Eaton, N. R. *Biochim. Biophys. Acta* **1967**, *146*, 173.
(35) Parkin, D. W.; Horenstein, B. A.; Abdulah, D. R.; Estupinan, B.; Schramm, V. L. *J. Biol. Chem.* **1991**, *266*, 20658.

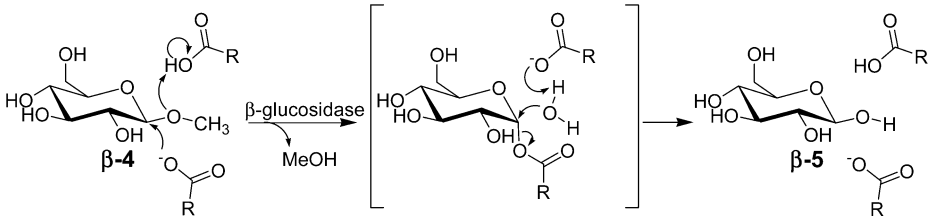

Figure 1. Reaction pathway for β-glucosidase, a retaining glycosidase. ***β*-4** undergoes nucleophilic attack from a carboxylate side chain, yielding a covalent α-acylal intermediate that then undergoes nucleophilic attack by water to yield ***β*-5**. The reaction pathway for α-glucosidase is essentially the same, but with the opposite anomeric stereochemistry.

ampicillin, and 17 mM potassium succinate as an internal standard for measuring the extent of reaction. Typically, 40 mg of solid α- or β-glucosidase was added to start the reaction, with a further 20−30 mg added if the reaction slowed. Reactions were followed with the reducing sugar assay until the reaction was ∼90% complete, approximately 10 days at 25 °C.

Extent of Reaction. Extents of reaction for calculating KIEs were determined accurately by NMR, with potassium succinate as an internal standard. For acid-catalyzed reactions, the 5 mL aliquot of $t = 0$ solution was cooled on ice and neutralized with 1 mL of 10 M KOH, added dropwise with stirring and cooling on ice. Precipitated $KClO_4$ was removed by filtration. The filtrate was concentrated under vacuum in a rotary evaporator. The process was repeated for 50 mL of the ∼90% reaction, neutralizing with 10 mL of 10 M KOH and filtering in a Buchner funnel. Both NMR samples were dissolved in D_2O, and the extent of reaction was determined by comparing the peak areas of the succinate methylene ($\delta_{CH2} = 34$ ppm) and C1 of **α-4** ($\delta_{C1} = 99$ ppm) or ***β*-4** ($\delta_{C1} = 105$ ppm).

Enzymatic Oxidation of Glucose. Each flask was brought to 10 mM potassium phosphate, pH 8.5, with solid potassium phosphate and adjusting the pH with KOH. Filtration was necessary for acid-catalyzed reactions, which were saturated in $KClO_4$. Glucose oxidase (20 mg, 3150 U), catalase (30 mg, 66 000 U), and 0.1% H_2O_2 were added, and the reactions were stirred uncovered overnight at 25 °C, quantitatively converting glucose to gluconic acid.

Anion Exchange Removal of Gluconic Acid. Reaction solutions were combined and reduced to 300 mL under vacuum. One-half was then applied to an anion exchange column (Dowex 1 × 4−200−400 mesh, 750 mL bed volume) in the acetate form. Flowthrough (300 mL) was discarded, and 80 × 10 mL fractions were collected with 100 mL/h flow. Fractions containing **4** were found by silica gel TLC in 1:1 MeOH: EtOAc and staining with 5% phosphomolybdic acid in EtOH (R_f = 0.6). The column was regenerated with 0.5 L of 3 M KCl, 1 L of dH_2O, 0.5 L of 3 M sodium acetate, and 1 L of dH_2O, and the procedure was repeated for the remaining reaction mixture. Fractions containing **4** were concentrated to dryness under vacuum.

Peracetylation of 4. Dried material from the previous step containing **4** and sodium acetate was combined with 30 mL of pyridine and 20 mL of acetic anhydride and stirred overnight at 25 °C, yielding **9** quantitatively. Solvent was removed under vacuum. Acetone (ca. 150 mL) was added and stirred for 1 h, and the salt precipitate was removed by filtration and washed with acetone until white. The filtrate was concentrated, the process was repeated with 50 mL of chloroform, and **9** was further purified by silica gel flash column chromatography in EtOAc. For unreacted **4**, which did not contain any sodium acetate, 1.0 g was added to 20 mL of pyridine and 30 mL of acetic anhydride, stirred overnight at room temperature, and then reduced to dryness.

NMR Experiments. Sealed NMR Tubes. Samples of **1** were flame sealed under vacuum in 5 mm NMR tubes.

***T*$_1$ Values.** T_1 values were measured by the inversion−recovery method for **α-9**, ***β*-9**, and **1** to determine the delay needed for excited nuclei to relax completely between radio frequency pulses.

Quantitative ^{13}C NMR. ^{13}C spectra for KIEs were acquired on a Bruker Avance 600 MHz NMR spectrometer using calibrated $\pi/2$ pulses, Waltz-super ^1H decoupling, a spectral width of 36 332 Hz, and a delay time between pulses, D_1, of 8.8 s for **9**, and 120 s for **1**[11] (10-times the longest T_1). Decoupling was applied only during acquisition to supress the NOE. Samples of **9** were prepared in d_6-acetone at a concentration of 50% (w/w). Samples were not spun during spectrum acquisition. There were 64k points per free induction decay (FID) with zero-filling to 256k. Spectra were recorded in 16 successive blocks of 256 scans (4096 scans total) and transformed separately.[36] Intensities were measured by integrating the spectra (i.e., based on peak area). The wide wings of the natural Lorentzian line shape could have caused overlap of closely spaced peaks in spectra of **9**. To avoid this, a Gaussian apodization was used with **9** with the parameters LB = −0.06 and GB = 0.01 in Bruker's XWINNMR program. These parameters preserved the intensity of the line but narrowed the line shape near the baseline. It was used also with **1** to allow comparison with previously determined KIEs. Peak integrations are sensitive to the early points of the FID; these parameters ensure that these points are not disturbed, yet the peak is still broad enough to be integrated reliably. ^{13}C peaks were quantitated by integration in the region ±5.0 Hz about the center of each peak. In a given experiment, the first block of 256 scans was integrated manually, and then the same integration regions were applied automatically to the remaining 15 blocks. For **1**, Lorentzian apodization functions were also used, with LB = 1. Quantitation by peak heights was also attempted with **1** using LB values as high as 20 Hz.

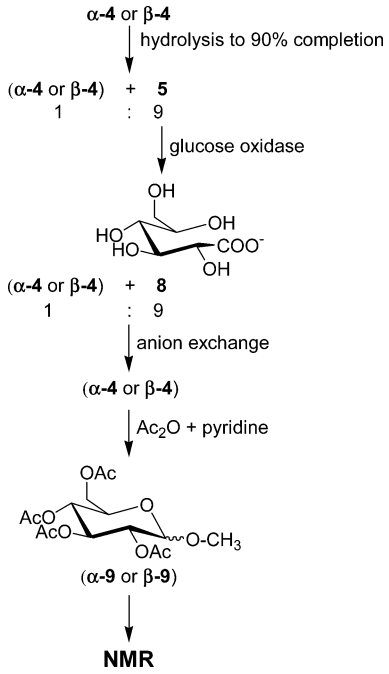

Experimental KIEs. Experimental KIEs were calculated from peak areas by first normalizing each peak area relative to C4 of **9** (or C5 of **1**) to give $R_{Cn} = (I_{Cn}/I_{C4})$, where I_{Cn}, I_{C4} are the integrated peak areas

(36) Bain, A. D.; Fahie, B. J.; Kozluk, T.; Leigh, W. J. *Can. J. Chem.* **1991**, *69*, 1189.

for carbon atoms n and 4. KIEs were then calculated as[11]

$$\mathrm{KIE}_{Cn} = \frac{\ln(1-F)}{\ln[(1-F)\times R_{i,Cn}/R_{0,Cn}]} \quad (1)$$

where KIE_{Cn} is the KIE for atom Cn, $R_{i,Cn}$ and $R_{0,Cn}$ are isotope ratios in **9** at times i and 0, and F is the fractional extent of reaction ($F = [\mathbf{4}]_i/[\mathbf{4}]_0$).

Calculated Equilibrium Isotope Effects. Equilibrium isotope effects (EIEs) were obtained from quantum mechanically optimized structures of **4** and **7**, and the corresponding vibrational frequencies. Optimizations and frequency calculations were performed with Gaussian 98[37] at the RB3PW91/6-31+G** level of theory, that is, density functional theory (DFT) with Becke's exchange functional[38] and Perdew and Wang's correlation functional.[39] Frequency scaling was not used. Initial optimizations were often performed at the RHF/3-21G** level of theory.

Fractionation factors (ϕ) at 298 and 353 K were calculated using QUIVER[40] for each optimized structure. ^{13}C EIE_{calc}'s were calculated by dividing the fractionation factors for **4** by **7**, that is, $\mathrm{EIE}_{calc} = \phi_4/\phi_7$. All ^{13}C EIE_{calc}'s were normalized relative to C4 so they were directly comparable with the experimental KIEs.

To examine the effects of ring conformation, different conformers were sought for **α-4** and ***β*-4**. Starting structures with ring conformations that were expected to be stable were optimized at a low level of theory (RHF/3-21G**) with the sugar ring dihedral angles fixed, then the constraints were released, and a full optimization was performed before changing to DFT.

Stable **7** ring conformations were sought, starting from different ring conformers of **α-4** and ***β*-4**, by fixing the C1−O bond at increasing bond lengths, corresponding to Pauling bond orders[41] $n_{C1-O} = 0.7-0.1$, and reoptimizing the rest of the structure at each fixed bond length. After optimization at $n_{C1-O} = 0.1$, the leaving group was removed altogether, and **7** was fully optimized. The E_4 conformer was also found, which did not proceed directly from any **4** conformer.

Results

Diels−Alder KIEs. KIEs were measured for the Diels−Alder reaction reported previously[11] to determine whether accurate KIEs could be obtained with Gaussian multiplication, as compared with the more commonly used exponential multiplication. KIE_{expt}'s determined in this work were within 0.001 of the literature values with exponential multiplication, and within 0.002 using Gaussian multiplication (see Supporting Information). Gaussian multiplication was therefore used in all **9** spectra because the narrower width at the base of the peak allowed baseline resolution of all ^{13}C peaks.

(37) Frisch, M. J.; Trucks, G. W.; Schlegel, H. B.; Scuseria, G. E.; Robb, M. A.; Cheeseman, J. R.; Zakrzewski, V. G.; Montgomery, J. A.; Stratmann, R. E.; Burant, J. C.; Dapprich, S.; Millam, J. M.; Daniels, A. D.; Kudin, K. N.; Strain, M. C.; Farkas, O.; Tomasi, J.; Barone, V.; Cossi, M.; Cammi, R.; Mennucci, B.; Pomelli, C.; Adamo, C.; Clifford, S.; Ochterski, J.; Petersson, G. A.; Ayala, P. Y.; Cui, Q.; Morokuma, K.; Malick, D. K.; Rabuck, A. D.; Raghavachari, K.; Foresman, J. B.; Cioslowski, J.; Ortiz, J. V.; Stefanov, B. B.; Liu, G.; Liashenko, A.; Piskorz, P.; Komaromi, I.; Gomperts, R.; Martin, R. L.; Fox, D. J.; Keith, T.; Al-Laham, M. A.; Peng, C. Y.; Nanayakkara, A.; Gonzalez, C.; Challacombe, M.; Gill, P. M. W.; Johnson, B. G.; Chen, W.; Wong, M. W.; Andres, J. L.; Head-Gordon, M.; Replogle, E. S.; Pople, J. A. *Gaussian 98*, revision A.6; Gaussian, Inc.: Pittsburgh, PA, 1998.
(38) Becke, A. D. *Phys. Rev. A* **1988**, *38*, 3098.
(39) Perdew, J. P.; Wang, Y. *Phys. Rev. B* **1992**, *45*, 13244.
(40) Saunders, M.; Laidig, K. E.; Wolfsberg, M. *J. Am. Chem. Soc.* **1989**, *111*, 8989.
(41) Pauling bond order n_{ij} between atoms i and j is defined as $n_{ij} = \exp\{(r_1 - r_{ij})/0.3\}$, where r_{ij} is the bond length between atoms i and j and r_1 is the bond length for a single bond between atoms of elements i and j (Johnston, H. S. *Gas-Phase Reaction Rate Theory*; Ronald Press: New York, 1966. Sims, L. B.; Lewis, D. E. In *Bond Order Methods for Calculating Isotope Effects in Organic Reactions*; Buncel, E., Lee, C. C., Eds.; Elsevier: New York, 1984; Vol. 6, p 161).

Table 1. Steady-State Kinetic Constants for Enzyme-Catalyzed **4** Hydrolyses[a]

enzyme	substrate	k_{cat} (s^{-1})	k_{cat}/K_M ($M^{-1}\,s^{-1}$)	K_M (mM)
α-glucosidase (recombinant, *S. cerevisiae*)	**α-4**	0.88 ± 0.05	15 ± 0.2	61 ± 9
β-glucosidase	***β*-4**	0.90 ± 0.15	2.0 ± 0.6	440 ± 13

[a] The kinetic constants k_{cat} and k_{cat}/K_M were calculated assuming that the enzymes were 100% active, with the concentration of active enzyme taken as the protein concentration.

Quantitation based on peak heights was also attempted, but it was accurate only in the extreme of very large peak widths with exponential multiplication (LB > 15 Hz). With **9**, such peak widths would have given extensive peak overlap and would therefore have been unusable (data not shown).

KIEs Measurement Method. Conditions were found for reacting 30−40 mmol of **4** to 90% completion, and isolating residual **4** from a 10-fold excess of contaminants (the products). The glucose product was oxidized to gluconic acid with glucose oxidase and removed by anion exchange chromatography. Preliminary experiments indicated that oxidation with Br_2 under basic conditions would also be suitable (data not shown). Quantitative peracetylation of **4** to **9** was achieved by reacting **4** in acetic anhydride and pyridine, then removing both, plus acetic acid, under strong vacuum in a rotary evaporator. This gave a 99.4% yield of **α-9**, with no partially acetylated peaks visible in the ^{13}C spectra. **α-9** and ***β*-9** were dissolved in an equal mass of d_6-acetone, giving 1.5 M, close to the solubility limit. For the acid reactions, removing the 2 M $HClO_4$ was greatly simplified by the low solubility of $KClO_4$ in water, 55 mM. Neutralizing with KOH gave $KClO_4$ precipitate which was removed by filtration.

Acid-Catalyzed 4 Hydrolysis. The rate constants for acid-catalyzed hydrolysis measured here (**α-4**, 6.8×10^{-5} s^{-1}; ***β*-4**, 2.7×10^{-4} s^{-1}) were in reasonable agreement with previously measured rates under the same conditions (7.3×10^{-5} and 1.4×10^{-4} s^{-1}, respectively).[32] A deep orange color developed in the acid-catalyzed reactions when taken to 90% completion, presumably due to condensation reactions involving glucose. No extra peaks appeared in the NMR spectra, implying that the orange material was a mixture of species. Polyalcohols such as inositol and sorbitol did not produce the orange color. NMR quantitation of the extent of reaction based on the amount of glucose in the reaction mixture was essentially the same as using an internal standard; however, a succinate internal standard was used for all KIE measurements to avoid any potential error from glucose side reactions.

Enzyme-Catalyzed 4 Hydrolysis. Barley amylase and *Aspergillus niger* amyloglucosidase could not hydrolyze **α-4** and ***β*-4** appreciably. Yeast α-glucosidase and almond β-glucosidase were able to hydrolyze their respective substrates to 90% completion, although with low efficiency (Table 1). Because of the low catalytic efficiency, the large amounts of **α-4** required, and the high cost of recombinant yeast α-glucosidase, three of four KIE determinations were performed with partially purified yeast α-glucosidase. KIEs with pure recombinant α-glucosidase were indistinguishable from those with partially pure enzyme (see Supporting Information), arguing that the same enzyme was responsible for activity against **α-4** in the partially purified enzyme.

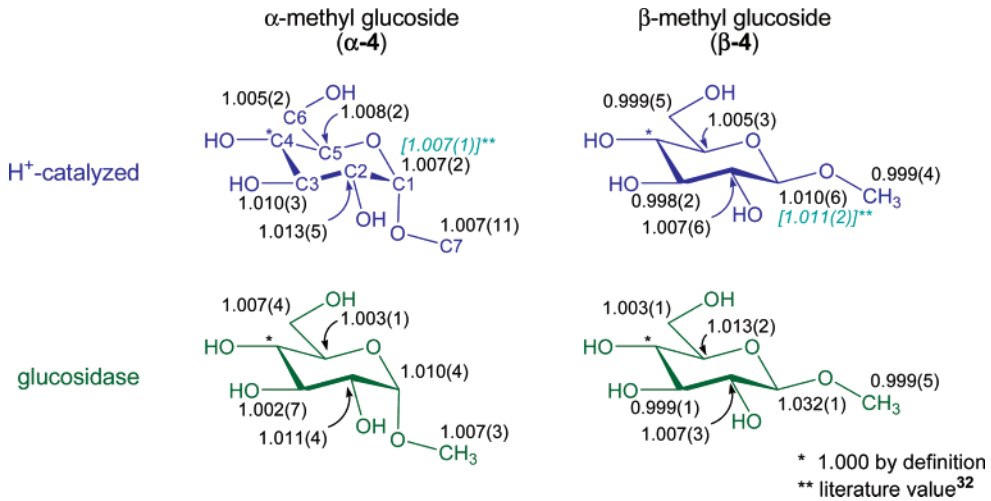

Figure 2. Experimental ^{13}C KIEs for acid-catalyzed (top row) and enzymatic (bottom row) hydrolysis of **α-4** and ***β*-4**. For α-glucosidase-catalyzed hydrolysis of **α-4**, there were four independent determinations of KIEs; the number in parentheses is the standard deviation in those measurements. For the other reactions, there were two independent KIE measurements. The average KIEs are reported, and the numbers in parentheses are the difference between the two measurements. Acid-catalyzed reactions were at 80 °C; enzymatic reactions were at 25 °C.

Experimental KIEs. ^{13}C KIEs were measured for every carbon atom in acid- and enzyme-catalyzed hydrolyses of **α-4** and ***β*-4** (Figure 2). There were four independent determinations of KIEs for the α-glucosidase reaction, and the errors reported are the standard deviations. For the other reactions, there were two independent KIE measurements, and the reported error is the difference between the two measurements. A standard deviation equal to one-half the reported difference would be expected if multiple measurements were made.

KIEs measured by the Singleton method are always relative to each other. For **4**, C4 was chosen as the reference atom because KIEs at this position were expected to be small, meaning that the reported relative KIEs would likely be close to the absolute KIEs. The similarity of the acid-catalyzed 1-^{13}C KIEs reported here to the previously reported values, which were absolute KIEs, supports this choice, as does the small absolute EIE_{calc}'s at C4, 0.999−1.003 (see below).

Calculated EIEs. Because the TSs of **4** hydrolysis were expected to be highly oxocarbenium ion-like, it is possible to compare the calculated equilibrium isotope effects (EIE_{calc}'s) on oxocarbenium ion formation with the experimental kinetic isotope effects (KIE_{expt}'s) of **4** hydrolysis, except at C1, which is a primary KIE.[42] EIE_{calc}'s between **4** and **7** were calculated for a variety of ring conformations in both the reactant and the oxocarbenium ion. Reasonable ring conformations for **7** were sought by starting from different stable **4** conformers ($^4C_1$, $^{2,5}B$, $B_{2,5}$, $^1S_3$) and constraining the C1−O bond at increasing lengths while reoptimizing the rest of the structure at each step. At a bond order of $n_{C1-O} = 0.1$, the leaving group was removed altogether, and **7** was fully optimized. One other conformer, E_4, was found which did not arise directly from **4**. Five stable conformers of **7** were found (Figure 3). Vibrational frequencies were used to calculate fractionation factors[43] (ϕ), and finally EIE_{calc}'s (see Supporting Information).

The effects of ring conformation on ϕ were modest for both **α-** and ***β*-4**. For ***β*-4**−**7**, the match of EIE_{calc}'s to KIE_{expt}'s was very good for all secondary KIEs (Figure 4b). For **α-4**−**7**, the best matches were for the E_3 and $^4H_3$ conformations of **7** (Figure 4a). The 3-^{13}C KIE_{expt} for the acid reaction was larger than EIE_{calc} for all combinations of **α-4** and **7** ring conformations. The 1-^{13}C KIE_{expt}'s were slightly higher than the EIE_{calc}'s for the **α-4** reactions and acid-catalyzed ***β*-4** hydrolysis, as expected for stepwise mechanisms where only the leaving group (in the D_N step) or the nucleophile (in the A_N step) is present in the reaction coordinate. The large 1-^{13}C KIE for β-glucosidase-

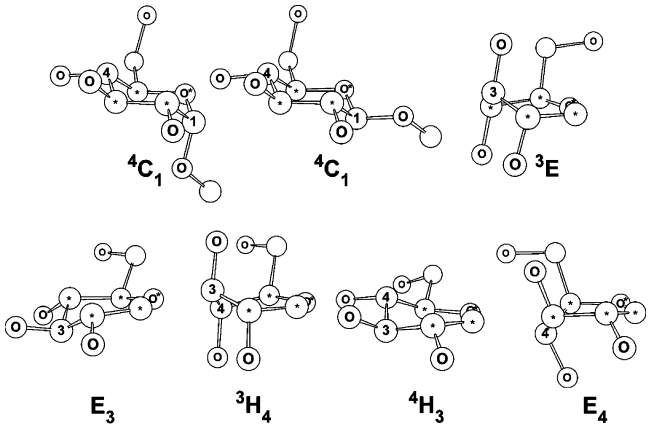

Figure 3. Sugar ring conformations. (top left, middle) $^4C_1$ conformers of **α-4** and ***β*-4**. (others) Stable conformers of **7** as found from DFT structure optimizations. The numbers of carbon atoms above or below the plane of the ring are shown, and coplanar atoms are marked (*). The $^3H_4$ conformer was distorted, with C3 further above the plane of the ring than C4 was below. Coordinates of these structures are given in the Supporting Information.

(42) KIEs include contributions from the change in molecular structure and from the reaction coordinate motion (leaving group departure and/or nucleophile approach). Reaction coordinate motion is expected to be significant for primary but usually not secondary ^{13}C KIEs. The structure of the sugar ring at the TS should be essentially an oxocarbenium ion; therefore, secondary KIEs should be essentially equal to the EIEs.

(43) Fractionation factors (ϕ) are, essentially, 1/EIE between the atom of interest and some reference state (Buddenbaum, W. E.; Shiner, V. J., Jr. In *Isotope Effects on Enzyme-Catalyzed Reactions*; Cleland, W. W., O'Leary, M. H., Northrop, D. B., Eds.; University Park Press: Baltimore, MD, 1977. Suhnel, J.; Schowen, R. L. In *Enzyme Mechanism from Isotope Effects*; Cook, P. F., Ed.; CRC Press: Boca Raton, FL, 1991). By using the same reference state for all values of ϕ, it is possible to estimate EIEs between different molecules. Experimentally derived values of ϕ normally use water or acetylene as reference states. Fractionation factors (and isotope effects) are vibrational phenomena that can be calculated in a straightforward way from quantum mechanically derived vibrational frequencies.[40] In this case, the reference state becomes a hypothetical, isolated atom. EIEs between corresponding atoms in **4** and **7** were calculated from the corresponding ϕ values.

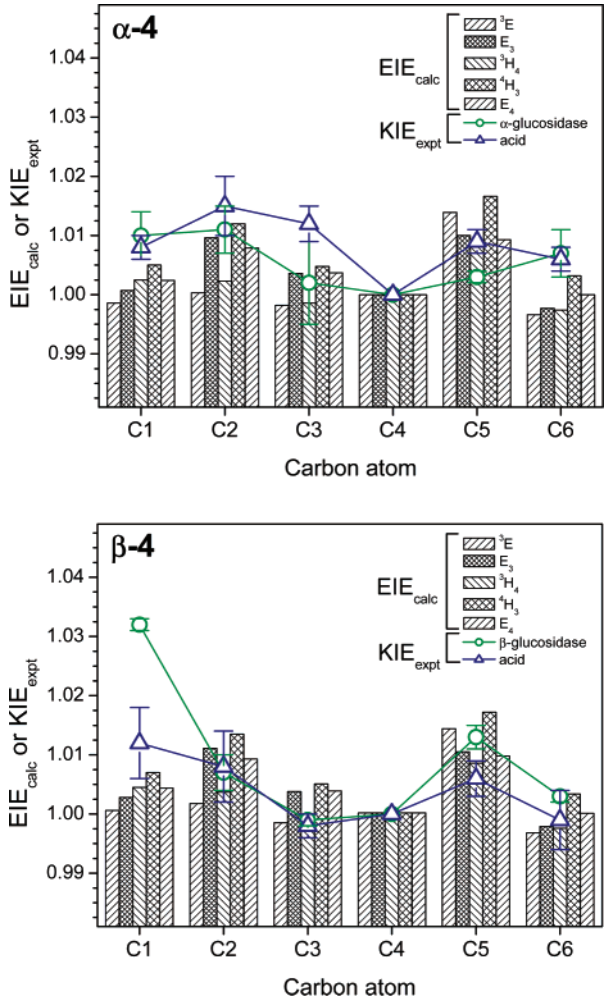

Figure 4. Comparison of EIE_{calc}'s with KIE_{expt}'s for (top) **α-4** and (bottom) ***β*-4** hydrolyses. EIE_{calc} values are shown as bars; KIE_{expt} values are shown as symbols. EIE_{calc}'s had $^4C_1$ ring conformations for **4**. Figure legends list the ring conformation for the oxocarbenium ions, **7**. For this figure only, the experimental acid-catalyzed KIEs, measured at 80 °C, were converted to 25 °C[44] for plotting on the same axes as enzymatic KIEs and calculated EIEs, all at 25 °C.

catalyzed ***β*-4** hydrolysis clearly indicates an A_ND_N mechanism, with both leaving group and nucleophile present in the reaction coordinate.

Discussion

Accuracy and Precision of Experimental KIEs. ^{13}C KIEs in this study matched previously reported values to within 0.001 for acid-catalyzed hydrolyses of **α-4** and ***β*-4** measured by the isotopic quasi-racemate method[32] (Figure 2) and to within 0.002 for the Diels−Alder reaction measured by NMR[11] (Table S1). The close match between the secondary KIE_{expt}'s and EIE_{calc}'s of oxocarbenium ion formation gives further confidence in the accuracy of the experimental KIEs.

KIEs on the α-glucosidase-catalyzed reaction had standard errors of 0.001−0.007 for four independent measurements, similar to the precision observed previously with scintillation counting or whole molecule mass spectrometry.[45−47] The precision of other KIE measurements, where there were two independent determinations, appeared to be similar.

Relative KIEs. NMR measurement gives KIEs which are relative to some reference atom, which has KIE = 1.000 by definition. C4 was chosen as the reference atom in **9** because it is the carbon atom furthest from the site of chemistry, and because the absolute 4-^{13}C EIE_{calc}'s were generally close to unity, with values of 0.999−1.003 for $^4C_1$ **α-** or ***β*-4** to E_3 or $^4H_3$ **7** (see Supporting Information). The choice of reference atom is not critical as long as all calculations use the same reference atom. However, it is helpful for qualitative interpretation that the relative KIEs be similar to the absolute values.

Speed. A major advantage of the NMR method is speed. It is not unusual to spend 2 years synthesizing a family of radiolabeled isotopologues for TS analysis. All of the experimental work to measure 28 ^{13}C KIEs in this study, including method development, was completed by one person (J.K.L.) in 20 months.

Competitive KIEs. Competitive KIEs were measured here, with all isotopomers present in the reaction, acting as competitive reactants. Competitive KIEs reflect steps up to and including the first irreversible step of the reaction, which for nonenzymatic reactions is generally the same as the rate-limiting step. Competitive KIEs report on k_{cat}/K_M for enzymatic reactions. With the glucosidase reactions, the first irreversible step was believed to be formation of the covalent acylal intermediate, based on the fact that the good substrates α- and *β-p*-nitrophenyl glucoside have k_{cat}'s of 18 and 20 s^{-1}, respectively,[48−50] as compared with <1 s^{-1} for **4** (Table 1). Thus, deglycosylation of the covalent glucosyl-enzyme intermediate (which is the same for *p*-nitrophenyl and methyl substrates) is much faster than k_{cat}'s for **4**. This implies that deglycosylation is much faster than glycosylation with **4**, making glycosylation effectively irreversible.

Commitment to Catalysis. It is normally necessary to measure commitment to catalysis when determining enzymatic KIEs. Commitment to catalysis occurs when an enzyme is so efficient that all or most of the enzyme·substrate complex partitions forward and undergoes catalysis rather than dissociating. In that case, the first irreversible step is substrate binding, and competitive KIEs do not reflect the chemical step. Commitment is normally measured by the isotope trapping method[51] with [enzyme] ≈ K_M, which was impossible with **4**, where K_M's were in the high millimolar range. Such high K_M's strongly imply weak substrate binding and no commitment to catalysis. The leaving group ^{18}O KIE for *β-p*-nitrophenyl glucoside with *β*-glucosidase[52] reflected the chemical step of the reaction, ensuring that the same will be true with ***β*-4**, a much worse substrate.

Transition State Analysis. It is well known by now that glycoside hydrolysis occurs through TSs with large amounts of oxocarbenium ion character.[3−5] Evidence for oxocarbenium ion-like TSs includes the effects of fluorine substitution in the sugar ring.[53−56] Fluorine, being electron withdrawing, decreases

(44) $KIE_{25\,°C} = \exp\{\ln(KIE_{80\,°C}) \times (353/298)\}$.
(45) Parkin, D. W. In *Enzyme Mechanism from Isotope Effects*; Cook, P. F., Ed.; CRC Press: Boca Raton, FL, 1991; p 269.
(46) Rosenberg, S.; Kirsch, J. F. *Biochemistry* **1981**, *20*, 3196.
(47) Berti, P. J.; Blanke, S. R.; Schramm, V. L. *J. Am. Chem. Soc.* **1997**, *119*, 12079.
(48) Dale, M. P.; Ensley, H. E.; Kern, K.; Sastry, K. A. R.; Byers, L. D. *Biochemistry* **1985**, *24*, 3530.
(49) Hansen, S. U.; Plesner, I. W.; Bols, M. *Chembiochem* **2000**, *1*, 177.
(50) Hosie, L.; Sinnott, M. L. *Biochem. J.* **1985**, *226*, 437.
(51) Rose, I. W. *Methods Enzymol.* **1980**, *64*, 47.
(52) Rosenberg, S.; Kirsch, J. F. *Biochemistry* **1981**, *20*, 3189.
(53) Mosi, R. M.; Withers, S. G. *Methods Enzymol.* **2002**, *354*, 64.

reaction rates by destabilizing the electron-deficient TS in proportion to its field effect on O5, the site with the greatest increase in charge in the oxocarbenium ion.[55] When excellent leaving groups, such as dinitrophenol, are combined with fluorine substitution, the effect on glycosylation is decreased while deglycosylation remains severely impaired, making it possible to trap covalent enzyme-sugar intermediates.[53,54] These have been used to demonstrate the covalent mechanisms of retaining enzymes, identify active site nucleophile carboxylates,[53,54] and solve crystal structures of covalent enzyme-bound intermediates.[57,58] Inhibition studies using cationic TS analogues that mimic an oxocarbenium ion have also contributed to the understanding of glycosidases.[4,5,59] Large α-^{2}H KIEs have been used as evidence for TSs with oxocarbenium ion character,[1] although the mechanistic utility of these KIEs has been questioned.[5]

More complete KIE studies have firmly established that glycoside hydrolyses tread the border between bimolecular A_ND_N and stepwise, unimolecular $D_N{*}A_N$ or $D_N + A_N$ mechanisms.[5,32,50,60−65] The details of enzymatic catalysis, including the location of catalytic residues, the importance of substrate ring conformation, and protonation trajectories, remain areas of intense research.[59,66] TS analysis using KIEs throughout the substrate can address these questions.

Acid-Catalyzed 4 Hydrolysis. Acid-catalyzed hydrolysis of various glucosides has been described as specific acid-catalyzed $D_N{*}A_N$, that is, stepwise and unimolecular.[1,32,67] The lifetimes of the oxocarbenium ions of glucose[67] and 2-deoxyglucose[68] in water, $\sim 10^{-12}$ s, are too short to diffusionally equilibrate with solvent. Analysis of ^{13}C, ^2H, and ^{18}O KIEs supports these conclusions.[32]

Ring Conformations. The 1-^{13}C KIE_{expt}'s measured here were the same, within experimental error, as those reported previously (Figure 2), helping to confirm the validity of our measurements. In the previous study, the 1-^2H, 2-^2H, and 4-^{18}O KIEs were interpreted as indicating a flattened $^1S_3$ ring conformation for the **α-4** TS, and $^4C_1$ flattened toward a $^4H_3$ half-chair for ***β*-4**.[32] The analysis of the ^2H KIEs hinged on the fact that they were smaller than EIEs expected for oxocarbenium ion formation based on calculations on methane diol at the RHF/4-31G level of theory. 2-^2H KIEs are sensitive to ring conformation because the KIE depends on hyperconjugation between the C2−H2 bond and the empty p-orbital of C1 in the oxocarbenium ion[69,70] and is dependent on the dihedral angle between the bond and the orbital. A small 2-^2H KIE is evidence for ring conformations that prevent good bond-orbital overlap. The 1-^2H KIEs were also smaller than expected for formation of **7**.

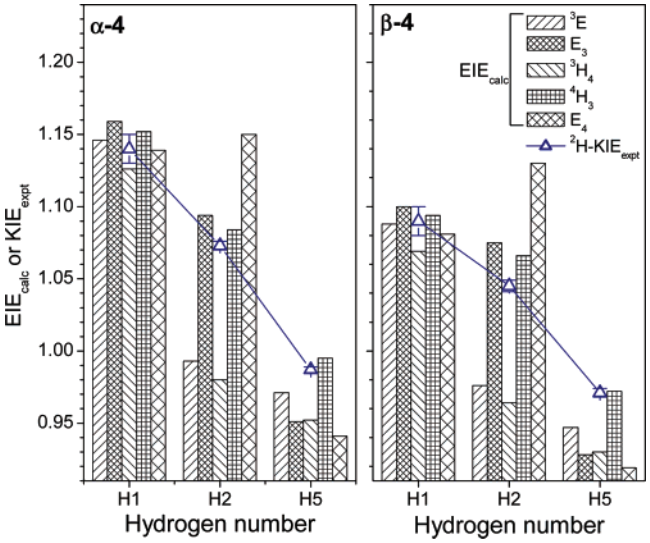

Figure 5. Comparison of EIE_{calc}'s with previously reported KIE_{expt}'s for acid-catalyzed hydrolyses of (left) **α-4** and (right) ***β*-4**. EIE_{calc} values are shown as bars; KIE_{expt} values are shown as symbols. KIE_{expt}'s and EIE_{calc}'s were all at 80 °C.

^{13}C EIE_{calc}'s. In this study, EIEs were calculated on the complete molecules, **4** and **7**, using a DFT method that is known to give high-quality vibrational frequencies.[71] A large number of ring conformations of **α-** and ***β*-4** and **7** were used to calculate EIEs (see Supporting Information). There was little difference in fractionation factors between different ring conformations of **4**, so the most likely conformer, $^4C_1$, was used as the reactant state. There was no single **7** ring conformation that unambiguously gave the best match of EIE_{calc}'s to the acid-catalyzed ^{13}C KIE_{expt}'s (Figure 4). For **α-4**, the E_3 and $^4H_3$ ring conformations gave the best match, although none of the EIE_{calc}'s matched the 3-^{13}C KIE_{expt}. For ***β*-4** hydrolysis, there was reasonably good agreement between KIE_{expt}'s and EIE_{calc}'s for all ring conformations.

^2H KIEs and EIEs. ^2H EIE_{calc}'s were also calculated and compared with the previously reported ^2H KIE_{expt}'s[32] (Figure 5). We found no evidence for distortion in the **7** ring structures. The α-secondary ^2H KIEs were not appreciably conformation-dependent, but did vary between **α-4** and ***β*-4**. Recent studies on EIE_{expt}'s for the anomeric equilibrium of glucose[72] showed that there was a significant difference in the vibrational environment of H1 in α- versus β-glucose, which was apparent as a 1-^2H $EIE_{expt} = 1.043$. This is reflected in the 1-^2H EIE_{calc}'s, where the **7** structures were the same and therefore the differences in EIE_{calc}'s arose from differences in **α-4** and ***β*-4**. The EIE_{calc}'s agreed well with the KIE_{expt}'s.

There was good agreement between 2-^2H KIE_{expt} for **α-4** and EIE_{calc} for the E_3 and $^4H_3$ conformations of **7**. These are the same conformations that matched best with the ^{13}C KIE_{expt}'s. For the ***β*-4** 2-^2H KIE_{expt}, the best match was also to the E_3 and $^4H_3$ conformations of **7**, although the EIE_{calc}'s were higher by

(54) Wicki, J.; Rose, D. R.; Withers, S. G. *Methods Enzymol.* **2002**, *354*, 84.
(55) Namchuk, M. N.; McCarter, J. D.; Becalski, A.; Andrews, T.; Withers, S. G. *J. Am. Chem. Soc.* **2000**, *122*, 1270.
(56) Konstantinidis, A.; Sinnott, M. L. *Biochem. J.* **1991**, *279*, 587.
(57) Vocadlo, D. J.; Davies, G. J.; Laine, R.; Withers, S. G. *Nature* **2001**, *412*, 835.
(58) Zechel, D. L.; Boraston, A. B.; Gloster, T.; Boraston, C. M.; Macdonald, J. M.; Tilbrook, D. M. G.; Stick, R. V.; Davies, G. J. *J. Am. Chem. Soc.* **2003**, *125*, 14313.
(59) Heightman, T. D.; Vasella, A. T. *Angew. Chem., Int. Ed.* **1999**, *38*, 750.
(60) Indurugalla, D.; Bennet, A. J. *J. Am. Chem. Soc.* **2001**, *123*, 10889.
(61) Zhang, Y.; Bommuswamy, J.; Sinnott, M. L. *J. Am. Chem. Soc.* **1994**, *116*, 7557.
(62) Tanaka, Y.; Tao, W.; Blanchard, J. S.; Hehre, E. J. *J. Biol. Chem.* **1994**, *269*, 32306.
(63) Huang, X. C.; Tanaka, K. S. E.; Bennet, A. J. *J. Am. Chem. Soc.* **1997**, *119*, 11147.
(64) Horenstein, B. A.; Bruner, M. *J. Am. Chem. Soc.* **1996**, *118*, 10371.
(65) Yang, J.; Schenkman, S.; Horenstein, B. A. *Biochemistry* **2000**, *39*, 5902.
(66) Vasella, A.; Davies, G. J.; Boehm, M. *Curr. Opin. Chem. Biol.* **2002**, *6*, 619.
(67) Amyes, T. L.; Jencks, W. P. *J. Am. Chem. Soc.* **1989**, *111*, 7888.
(68) Zhu, J.; Bennet, A. J. *J. Am. Chem. Soc.* **1998**, *120*, 3887.
(69) Sunko, D. E.; Szele, I.; Hehre, W. J. *J. Am. Chem. Soc.* **1977**, *99*, 5000.
(70) Matsson, O.; Westaway, K. C. *Adv. Phys. Org. Chem.* **1998**, *31*, 143.
(71) Wong, M. W. *Chem. Phys. Lett.* **1996**, *256*, 391.
(72) Lewis, B. E.; Schramm, V. L. *J. Am. Chem. Soc.* **2001**, *123*, 1327.

0.02−0.03. The reason for this discrepancy is not yet clear. The best match of 5-^{2}H EIE_{calc}'s occurred with the $^4H_3$ conformation, but isotope effects at this position have not been extensively characterized, so it would be premature to assign the **7** ring conformations on the basis of this isotope effect alone.

Ring Conformation at the Transition State. Based on the match of EIE_{calc}'s with KIE_{expt}'s, both **α-4** and ***β*-4** proceed through TSs with E_3 or $^4H_3$ conformations (Figure 3). In both conformations, C3 is located below the plane of the ring. The main difference is whether C4 is in the plane of the ring, as in E_3, or above it, as in $^4H_3$. This result is satisfying in that the dominant solution conformer of both **α-** and ***β*-4**, $^4C_1$, gave the E_3 conformer of **7** when the C1−O bond was computationally broken in steps. This indicates that the E_3 conformer of **7** is accessible from the reactants and that no unusual conformational changes or ring distortions are required. It may be possible to distinguish between the E_3 and $^4H_3$ conformers once all of the ^{2}H KIEs have been measured.

Previously, the **7** ring conformation was assigned as a flattened $^1S_3$ for **α-4** and $^4H_3$-like for ***β*-4**. Both of the previously assigned rings had C3 below the plane of the ring. Our analysis of ring conformation is based on structure and vibrational frequency calculations at levels of theory that were not accessible in 1986. The essential conclusions about ring conformation from the previous study remain intact, that ***β*-4** hydrolysis does not proceed through a boat conformation, in contradiction of the antiperiplanar lone pair hypothesis.[32]

Glucosidase-Catalyzed 4 Hydrolysis. 1-^{13}C KIE_{expt}'s have previously been reported for hydrolysis of α-glucopyranosyl fluoride (1.007, on k_{cat}/K_M) by sugar beet α-glucosidase,[62] and α-pyridinium (1.028, on k_{cat}) and α-isoquinolinium glucopyranosides (1.028, on k_{cat}) by yeast α-glucosidase.[63]

α-Glucosidase. The primary ^{13}C KIE with **α-4** was 1.010 ± 0.004, most consistent with a stepwise D_N*A_N mechanism. That is, a discrete oxocarbenium ion intermediate is formed in the active site of the enzyme between leaving group (methanol) departure and nucleophilic addition of the carboxylate side chain of the enzyme. This result is in contrast to the hydrolysis of pyridinium glucopyranosides by α-glucosidase, where 1-^{13}C KIEs of ∼1.027 on k_{cat} (i.e., C1−N bond cleavage) indicated an A_ND_N mechanism.[63] In the current study, KIEs on k_{cat}/K_M were measured, which reflect the first irreversible step of the reaction. It is likely that the rate-limiting and first irreversible steps are the same, glycosylation, so it is reasonable to compare the KIEs on the different kinetic constants. The difference in KIEs seems to indicate that the character of the TS (concerted vs stepwise) is not an intrinsic feature of a given enzyme and depends on enzyme/substrate interactions. More generally, it implies that the energetic difference between A_ND_N and D_N*A_N is modest. The observation that nonenzymatic glycoside hydrolyses proceeding through A_ND_N mechanisms (based on primary ^{13}C KIEs) can change to D_N*A_N mechanisms in enzyme-catalyzed hydrolyses (e.g., see ref 5) is consistent with a small energetic difference.

The pattern of secondary ^{13}C KIE_{expt}'s in the enzymatic reactions was different from the acid-catalyzed reaction of **α-4**, implying that α-glucosidase uses binding energy to alter the conformation of the sugar ring at the TS. Detailed interpretation of those conformational changes awaits measurement of the ^{2}H KIEs.

***β*-Glucosidase.** For β-glucosidase-catalyzed ***β*-4** hydrolysis, the KIE_{expt}'s were very similar to the acid-catalyzed reaction, except at C1 and C5. The significance of the 5-^{13}C KIE remains to be explained. The large 1-^{13}C KIE shows that β-glucosidase employs an A_ND_N mechanism. That is, nucleophilic attack by the active site carboxylate is concerted with leaving group departure. It was roughly equal to the 1-^{13}C KIEs for hydrolysis of pyridinium glucopyranosides by yeast α-glucosidase, as well as the spontaneous hydrolysis of α-glucopyranosyl fluoride[61] and acid-catalyzed hydrolysis of methyl 5-thioxylopyranosides.[60]

The similarities between the secondary ^{13}C KIEs for the enzyme- and acid-catalyzed reactions imply that the enzyme exerts little or no distortion on the sugar ring during catalysis. This is consistent with previous results which indicated relatively weak interactions with glucose and that it is indifferent to substitutions at C4 and C5.[3] The main β-glucosidase specificity determinants were in the aglycon portion of the substrate.[3,48] More detailed TS analysis of the β-glucosidase reaction awaits determination of all of the ^{2}H KIEs.

Conclusions

KIE measurement by the Singleton method, at natural abundance by NMR, is a tremendous improvement on previous methods that required synthesis of isotopologues and measurement of KIEs one at a time. We measured 28 ^{13}C KIEs on α- and β-methyl glucoside hydrolysis. The acid-catalyzed reactions proceeded by a stepwise D_N*A_N mechanism, with oxocarbenium ion intermediates in the E_3 or $^4H_3$ conformations. α-Glucosidase-catalyzed hydrolysis also proceeded through a stepwise D_N*A_N mechanism. The secondary ^{13}C KIEs showed that the sugar ring was distorted at the TS. The β-glucosidase reaction proceeded through a concerted A_ND_N TS, with no sign of sugar ring distortion. Determination of the ^{2}H KIEs will allow complete characterization of the enzymatic TSs.

Acknowledgment. We thank Dr. Don Hughes and Brian Sayer of the McMaster NMR facility for invaluable advice and assistance in this work. We also thank Dr. Andy Bennet (Simon Fraser University) for valuable discussions on the interpretation of α-secondary ^{2}H KIEs. This work was supported by the Natural Sciences and Engineering Research Council of Canada and a career award from the Canadian Institutes of Health Research (P.J.B.).

Supporting Information Available: Experimental KIEs, optimized structures, calculated EIEs, fractionation factors, NMR peak assignments (PDF). This material is available free of charge via the Internet at http://pubs.acs.org.

JA0394028